Coevolution Creates Complex Mosaics across Large Landscapes

Lucas D. Fernandes,[1,*] Paula Lemos-Costa,[2] Paulo R. Guimarães Jr.,[3] John N. Thompson,[4] and Marcus A. M. de Aguiar[5]

1. Department of Life Sciences, Imperial College London, Silwood Park, Ascot, Berkshire SL5 7PY, United Kingdom; 2. Programa de Pós-graduação em Ecologia, Instituto de Biologia, Universidade Estadual de Campinas, 13083-865 Campinas, São Paulo, Brazil; and Department of Ecology and Evolution, University of Chicago, Chicago, Illinois 60637; 3. Departamento de Ecologia, Universidade de São Paulo, 05508-090 São Paulo, São Paulo, Brazil; 4. Department of Ecology and Evolutionary Biology, University of California, Santa Cruz, California 95060; 5. Instituto de Física "Gleb Wataghin," Universidade Estadual de Campinas, 13083-859 Campinas, São Paulo, Brazil

Submitted June 3, 2018; Accepted March 14, 2019; Electronically published June 21, 2019

Online enhancements: appendix, videos.

ABSTRACT: The spatial distribution of populations can influence the evolutionary outcome of species interactions. The variation in direction and strength of selection across local communities creates geographic selection mosaics that, when combined with gene flow and genomic processes such as genome duplication or hybridization, can fuel ongoing coevolution. A fundamental problem to solve is how coevolution proceeds when many populations that vary in their ecological outcomes are connected across large landscapes. Here we use a lattice model to explore this problem. Our results show that the complex interrelationships among the elements of the geographic mosaic of coevolution can lead to the formation of clusters of populations with similar phenotypes that are larger than expected by local selection. Our results indicate that neither the spatial distribution of phenotypes nor the spatial differences in magnitude and direction of selection alone dictate coevolutionary dynamics: the geographic mosaic of coevolution affects formation of phenotypic clusters, which in turn affect the spatial and temporal dynamics of coevolution. Because the formation of large phenotypic clusters depends on gene flow, we predict that current habitat fragmentation will change the outcomes of geographic mosaics, coupling spatial patterns in selection and phenotypes.

Keywords: antagonisms, geographic mosaic of coevolution, mutualisms, phenotypic patterns, selection patterns, species interactions.

Introduction

One of the main questions at the interface of evolution and ecology is how species interactions shape the diversity of life (Thompson 2005). Evolution mediated by species interactions may influence speciation rates (Johnson 2010), extinction rates (van Valen 1973), spatial distributions (Alonso et al. 2002), community organization (Gotelli et al. 2010; Nuismer et al. 2013), and genetic (Wade 2007) and phenotypic (Guimarães et al. 2017) diversity. Deciphering how species interactions shape evolutionary rates and patterns, however, has been challenging, because each interaction between a pair of species is a collection of local interactions that may vary in ecological outcomes and fitness effects on the participants (Brodie et al. 2002; Gandon et al. 2008). The geographic mosaic theory of coevolution confronts this complexity by considering relationships between species as genotype-by-genotype-by-environment (G × G × E) interactions (Thompson 2005).

The sources of spatial variation can be partitioned into three main components that affect G × G × E interactions and the resulting coevolutionary dynamics. First, the direction and magnitude of selection can vary across local communities, creating geographic selection mosaics (Brodie et al. 2002; Parchman and Benkman 2002). For example, *Greya* moths are major pollinators of woodland star (*Lithophragma*) flowers that lay eggs in the same flowers that they pollinate. The larvae eat very few seeds, and the interaction is mutualistic in many environments. In some environments, however, the presence of copollinators that do not lay eggs in the flowers swamp the mutualism, making the interaction between the plants and *Greya* moths antagonistic rather than mutualistic (Thompson and Cunningham 2002). Second, reciprocal selection may vary among environments, creating coevolutionary hotspots, where the interaction affects the fitness of both partners, and coevolutionary coldspots, where selection is not reciprocal or there is no selection (Laine 2009). Finally, gene flow, hybridization, and genomic alterations can lead to trait remixing among populations as allele frequencies and the structure of genomes undergo continual reorganization in different ways in different populations (Whitham et al. 2006; Thompson and Merg 2008; Lexer et al. 2013). Trait remixing results in variation among populations in the phenotypic distribution of traits available for natural selection (Dybdahl and Lively 1996).

* Corresponding author; email: lucasdf.phys@gmail.com.

ORCIDs: Fernandes, https://orcid.org/0000-0001-6053-2277; Lemos-Costa, https://orcid.org/0000-0001-6983-2022; de Aguiar, https://orcid.org/0000-0003-1379-7568.

Am. Nat. 2019. Vol. 194, pp. 217–229.
DOI: 10.1086/704157

Collectively, selection mosaics, coevolutionary hotspots, and trait remixing can fuel ongoing coevolution in ways that differ from solely local coevolution in rates, trajectories, and patterns of phenotypic change (Nuismer et al. 1999).

The dynamics of coevolutionary mosaics have now been explored in mathematical models (Nuismer et al. 1999; Gibert et al. 2013; Lemos-Costa et al. 2017), laboratory microcosms (Forde et al. 2004; Vogwill et al. 2009), and natural communities (Parchman and Benkman 2002; Gómez et al. 2009; Gómez and Buckling 2011), but most studies have been limited to analysis of few populations relative to the full spatial complexity found in assemblages of coevolving species in nature. These studies, however, have shown that all three components of coevolutionary mosaics can contribute to discrepancies between the local patterns of natural selection and the local distribution of phenotypes. For example, at the local level, theory predicts that mutualisms would favor fixation of beneficial phenotypes, whereas antagonistic interactions may show unbounded oscillations of phenotype frequencies (Nuismer et al. 1999). In contrast, if an interaction is distributed across two ecologically contrasting sites linked by gene flow, mutualisms may not result in fixation of beneficial alleles at the local level and antagonisms may show damped oscillations of phenotypes or long-lasting clines along linear arrays of populations (Nuismer et al. 1999, 2000; Gomulkiewicz et al. 2000). Taken together, the available studies of coevolutionary dynamics indicate that spatial structuring results in qualitatively different outcomes than predicted by studies at single sites (Gibert et al. 2013; Lion and Gandon 2015; Lemos-Costa et al. 2017).

A current major problem to solve is how the consequences of the spatial organization of interactions scale up across large landscapes formed by hundreds or thousands of ecologically different sites rather than just a few sites (Thompson 2005). That is, how do the spatial scales of coevolutionary selection and gene flow shape the spatial scales of evolutionary outcomes? Here we integrate coevolutionary models, numerical simulations, and tools derived from statistical mechanics to evaluate how coevolution proceeds between species whose interactions vary from antagonism to mutualism across environmentally diverse landscapes. We show that coevolution across many ecologically diverse sites creates patterns in the distribution of coevolving traits that cannot be predicted by local selection alone or by models assuming simpler spatial organization. Specifically, we show that the interplay between selection mosaics, coevolutionary hotspots and coldspots, and trait remixing across large landscapes lead to the formation of regional groups of populations characterized by similar phenotypes that are larger than expected by the patterns of selection at local levels alone. The results show that complex patterns of trait matching and mismatching occur through the combined effects of selection mosaics and gene flow among coevolutionary hotspots. In addition, we show that these patterns may have statistical properties that are predictable and thus may be explored with empirical data.

Methods

Model

We consider an $L \times L$ square lattice with periodic boundary conditions where each site represents a community with two species. Individuals of the two different species interact within sites, and interactions can be mutualistic or antagonistic depending on the site. Each site, however, is linked to its nearest neighbors, and individuals of both species can migrate to connected sites. The sites are labeled (i, j) with $i, j = 1, 2, \ldots, L$. Following Nuismer et al. (1999), we model the species as haploid individuals and consider the interactions to be governed by a single locus with two alleles. As local populations are considered infinite, the dynamics act on the allelic frequencies, which is a reasonable simplifying assumption grounded in classical population genetics (Rice 2004). Species X, referred to as symbiont, has alleles A and a, with x_{ij} denoting frequency of allele A at site (i, j), and species Y, referred to as host, has alleles B and b, with y_{ij} denoting frequency of allele B at site (i, j). The symbiont always receives a fitness increase when interacting with matching alleles (A matches B and a matches b; there are no cross interactions). Fitness increases or decreases for the host depend on the site. For the sites where the interaction between the species is mutualistic (hereafter, mutualistic sites or mutualistic selection), the fitness of the host increases for matching alleles. Otherwise, for the sites where the interaction is antagonistic (hereafter, antagonistic sites or antagonistic selection), the fitness decreases for the host species when alleles are matched. For these analyses, we use the concepts of genotype and phenotype interchangeably, or in other words, we consider a direct relation between allele frequencies and corresponding traits (no environmental influence of the phenotypes). The selection mosaics are established at the beginning of the simulation and held fixed throughout the simulation. Each site is assigned as mutualistic with probability p and antagonistic with probability $(1 - p)$. Population fitnesses are modeled according to

$$\begin{aligned} W_A^{(i,j)} &= 1 + Qy_{ij}, \\ W_a^{(i,j)} &= 1 + Q(1 - y_{ij}), \\ W_B^{(i,j)} &= 1 + \gamma_{ij}x_{ij}, \\ W_b^{(i,j)} &= 1 + \gamma_{ij}(1 - x_{ij}), \end{aligned} \tag{1}$$

where $W_\alpha^{(i,j)}$ is the fitness of allele α at site (i, j) and Q is the sensitivity of the fitness of the symbiont to changes in the allelic frequency of the host. Note that as the symbiont always receives a fitness increase from the interaction, $Q > 0$. The pa-

rameter γ_{ij} represents the sensitivity of the fitness of the host to changes in the allelic frequency of the symbiont, and its value depends on the type of local interaction. We set $\gamma_{ij} = K_M > 0$ for sites with mutualistic interactions, in which interaction between matching alleles increases the host's fitness, and $\gamma_{ij} = K_A < 0$ for sites with antagonistic interactions, in which interaction decreases the host's fitness. We refer to K_M and K_A as the strengths of selection for mutualism and antagonism, respectively. Gene flow happens before selection with rate m, equally divided among the four nearest neighbors. With these assumptions, we have the following recurrence equations for the changes of frequencies x_{ij} and y_{ij} in each generation:

$$\begin{aligned} x_{ij}^{(n+1)} &= \frac{x_{ij}^{(n,*)} W_A^{(i,j)}}{x_{ij}^{(n,*)} W_A^{(i,j)} + (1 - x_{ij}^{(n,*)}) W_a^{(i,j)}}, \\ y_{ij}^{(n+1)} &= \frac{y_{ij}^{(n,*)} W_B^{(i,j)}}{y_{ij}^{(n,*)} W_B^{(i,j)} + (1 - y_{ij}^{(n,*)}) W_b^{(i,j)}}, \end{aligned} \tag{2}$$

where

$$\begin{aligned} x_{ij}^{(n,*)} &= x_{ij}^{(n)}(1 - m) + \frac{m}{4} \sum_{(s,t)} x_{i+s,j+t}^{(n)}, \\ y_{ij}^{(n,*)} &= y_{ij}^{(n)}(1 - m) + \frac{m}{4} \sum_{(s,t)} y_{i+s,j+t}^{(n)} \end{aligned} \tag{3}$$

are the allelic frequencies after gene flow (the summations over s and t are restricted to the four nearest neighbors). Note that the choice of local infinite population sizes provides a simplification that eliminates fluctuations from stochastic effects such as genetic drift, allowing the investigation of the effect of species interaction and coevolution in generating phenotypic patterns at the landscape scale in the absence of complicating factors. In all simulations, both x and y are initiated with values 0.51 for every site on the lattice, so that the differences in the phenotypic patterns arise due to spatial variation in the local interaction and to gene flow, not to variation in initial conditions among sites. The square lattice has size $L = 100$, and evolution occurs for 40,000 generations.

Mean Field with Spatially Varying Carrying Capacities

The balance between spatial prevalence of one interaction and local selection strength was further explored with a mean-field, two-site approximation, in which each site has a carrying capacity representing the spatial prevalence over the landscape (parameters p for mutualistic sites and $(1 - p)$ for antagonistic sites in the landscape model).

The two-site model proposed by Nuismer et al. (1999) was modified to include different carrying capacities associated with each site (Lemos-Costa et al. 2017). Specifically, we consider the situation in which the first site, where the interactions are mutualistic, has carrying capacity N_1, whereas the second site, where the interactions are antagonistic, has carrying capacity N_2. In this case, the equations describing the gene flow between the sites change to

$$\begin{aligned} x_1^{(n,*)} &= \frac{x_1^{(n,*)}(1 - m)N_1 + x_2^{(n,*)} m N_2}{(1 - m)N_1 + m N_2}, \\ x_2^{(n,*)} &= \frac{x_2^{(n,*)}(1 - m)N_2 + x_1^{(n,*)} m N_1}{(1 - m)N_2 + m N_1}. \end{aligned} \tag{4}$$

These equations can be rewritten as

$$\begin{aligned} x_1^{(n,*)} &= \frac{x_1^{(n,*)}(1 - m)R + x_2^{(n,*)} m}{(1 - m)R + m}, \\ x_2^{(n,*)} &= \frac{x_2^{(n,*)}(1 - m) + x_1^{(n,*)} m R}{(1 - m) + m R}, \end{aligned} \tag{5}$$

which depend only on the ratio $R = N_1/N_2$ between the carrying capacities of the mutualistic and antagonistic communities. We tested eight different values of R, going from $R = 1$ to $R = 0.3$ in intervals of 0.1. The equations for y_1 and y_2 are given by equivalent expressions. The selection equations are the same as the ones for the two-site model (Nuismer et al. 1999).

To compare the results of the mean-field approach with the simulations on the lattice, we define the variable C_j, which describes the behavior of the frequency of allele A (x_j) for each community j:

$$C_j = 2(x_j - 0.5). \tag{6}$$

When allele A is fixed or close to fixation ($x \approx 1$), the community presents genotypic patterns in accordance with an isolated mutualistic community and $C \approx 1$. When the allele A is close to 0.5, it presents the pattern expected from an isolated antagonistic community and $C \approx 0$. Fixation of allele a ($x \approx 0$) would give $C \approx -1$. Finally, to compare the mean-field results with the spatial prevalence of mutualistic versus antagonistic communities in numerical simulations, we calculate the average value C_{av}, which considers the size of each community:

$$C_{\text{av}} = \frac{N_1}{N_1 + N_2} C_1 + \frac{N_2}{N_1 + N_2} C_2. \tag{7}$$

The size of each community in the mean-field model is comparable to the number of sites with each local outcome of selection (mutualistic vs. antagonistic) in the spatial model. Given that the parameter p is approximated by the frequency of mutualistic sites on the lattice, $p = N_M/(N_M + N_A)$, with N_M and N_A the numbers of mutualistic and antagonistic sites, respectively, and defining $R = N_M/N_A$, we have

$$R = \frac{p}{1 - p}. \tag{8}$$

Thus, we can compare the ratio of the carrying capacities (R) and the probability of a given site to be mutualistic on the lattice (p), which are the determinants of the behavior transitions in their respective models, and check how well the mean field describes the evolutionary outcomes on the spatial lattice.

Cluster and Coldspots Analyses

To count clusters of a given allele frequency, we first define a frequency interval. For example, when counting clusters where the frequency of allele A is larger than 0.7, we start with a site where the allele frequency is in the selected interval. Next, the four nearest neighbors of that site are analyzed, and if their allelic frequency also belongs to that interval, they are added to the cluster. The neighbors of the neighbors are all analyzed, until no other sites are added, indicating the end of the process. This iteration is repeated until all sites on the lattice are visited. Isolated sites (for which none of the four neighbors belong to the same interval) are considered clusters of size one. This process gives the numbers of clusters with all sizes in the chosen interval. Finally, we normalize the distributions by the total number of clusters found for a given value of gene flow.

For the coldspots analysis, the selection mosaics are first built the same way as before, with each site assigned as mutualistic with probability p and antagonistic with probability $(1 - p)$. A given fraction f of the sites is then chosen randomly and marked as coldspots, where the interaction favors the symbiont (with fitness effects being the same as in hotspots; i.e., $Q > 0$), but does not influence the host's fitness (at coldspots, we have $\gamma_{ij} = 0$ and $W_B = W_b = 1$). This process, however, changes the average fitness sensitivity of the host, $\overline{s_{Y^C}} = (1/L^2)\Sigma_{ij}\gamma_{ij}$, as the fraction of coldspots is increased (see the appendix, available online). To keep the average fitness sensitivity fixed as the fraction of coldspots is varied, the value of p for the initial selection mosaic has to be a function of f. Thus, for a fixed average fitness sensitivity of the host, $\overline{s_{Y^C}}$, for each value of f to be tested, the value of p is defined as

$$p = \frac{1}{(K_M - K_A)}\left[\frac{\overline{s_{Y^C}}}{(1-f)} - K_A\right]. \tag{9}$$

Results

Spatial Patterns for Alleles A and B

Our analysis suggests that coevolutionary mosaics in large landscapes lead to unexpected large-scale phenotypic patterns that cannot be explained by local processes alone. The transient evolutionary trajectories produced pockets of high allele frequency, and after a few thousand generations the spatial patterns stabilized and became stationary. We begin our analysis with the stationary patterns of allele A and B frequencies (symbiont and host species, respectively) across the landscape.

We first explored how gene flow affects the distribution of allele A frequencies when mutualism increasingly dominates the landscape. In these scenarios, we varied the proportion of mutualistic sites, keeping the intensity of selection fixed and twice as high for the host species in mutualistic sites than in antagonistic sites ($|K_M| = 2|K_A|$). Under these conditions, different combinations of selection mosaics and gene flow resulted in substantially different large-scale spatial patterns of allele A distributions (fig. 1). Although we have iterated the process for 40,000 generations, to guarantee stationarity for all parameter sets, the majority of sites on the landscape settled on the final allele frequencies much earlier (in many cases, before 3,000 generations; see videos A2 and A3 in the appendix). At low rates of gene flow ($m = 0.002$; fig. 1*b*, 1*f*, 1*j*), the spatial distribution of frequency of alleles mirrored the distribution expected by the local pattern of selection: antagonistic sites maintained polymorphic populations, whereas mutualistic sites showed allele fixation. When the proportion of antagonistic sites was higher than that of mutualistic sites ($p = 0.25$), the spatial prevalence of antagonistic sites compensated for the stronger intensity of selection at mutualistic sites. As a result, polymorphism remained prevalent throughout the landscape (fig. 1*d*).

Large and stable regional groups of high allele frequencies developed as the proportion of mutualistic sites and gene flow increased. These stable clusters of high allele frequencies locally shielded those sites from the oscillatory dynamics generated by local antagonistic selection (fig. 1*d*). As the proportion of mutualistic sites and the rate of gene flow increased, the landscape began to appear as if mutualism were ubiquitous, even though the interaction was antagonistic at some sites (fig. 1*h*, 1*l*). The effects of cluster shielding and consequent loss of resolution of fine structures on the mosaic can be further investigated if we consider ordered structures for the spatial distribution of antagonistic and mutualistic sites. Block and gradient mosaics are useful to understand how gene flow affects allele clines on the boundary of different selection regions, as well as how gene flow and selection mosaic clusters influence the loss of resolution of spatial structures on the final phenotypic patterns (see the appendix).

The stationary distributions for allele B frequencies reveal similar patterns, obtained with the same underlying spatial structure of selection mosaics and the same parameters as before but with important differences. At low rates of gene flow ($m = 0.002$; fig. 2*b*, 2*f*, 2*j*), the spatial distribution of allele frequencies leads to allele fixation at mutualistic sites and polymorphism at antagonistic sites. The most striking differences in comparison with the patterns for allele A appear as gene flow increases. When antagonistic sites are common

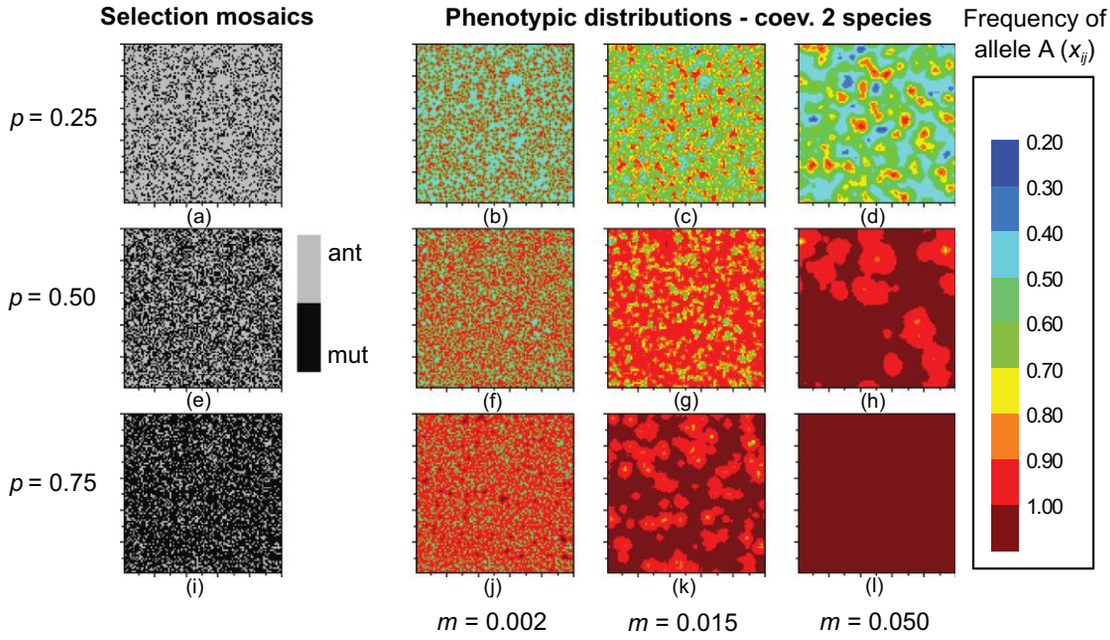

Figure 1: Final stationary patterns of x (frequency of allele A) for three values of the gene flow rate, m, and different selection mosaics (each mosaic defined by the probability of a site to be mutualistic, p). The three final patterns in each row correspond to the same selection mosaic on the left. The other parameters are $K_M = 0.04$, $K_A = -0.02$, and $Q = 0.02$, and each pattern is iterated over 40,000 generations. ant = antagonistic; mut = mutualistic.

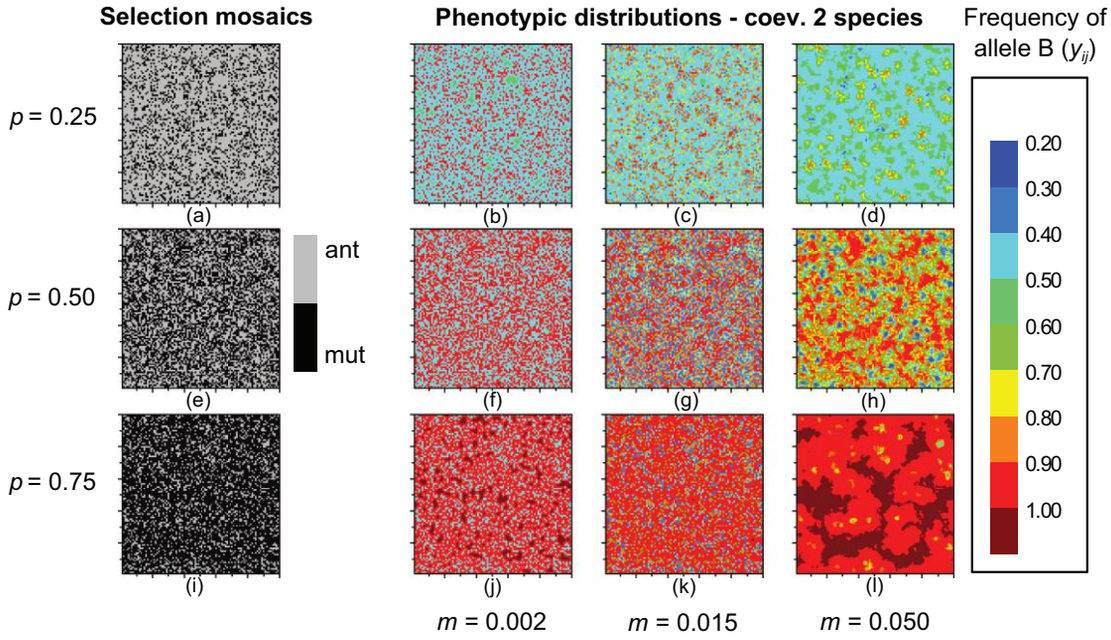

Figure 2: Final stationary patterns of y (frequency of allele B) for three rates of gene flow, m, and different selection mosaics (each mosaic defined by the probability of a site to be mutualistic, p). Patterns correspond to the coevolutionary model (both x and y vary in time). Selection mosaics and parameters are the same as in figure 1. Each simulation ran for 40,000 generations. ant = antagonistic; mut = mutualistic.

($p = 0.25$), a high level of gene flow ($m = 0.050$; fig. 2*d*) also maintains a polymorphic state throughout the landscape. In contrast to the patterns observed for allele *A*, the characteristic sizes of the clusters where the frequency of allele *B* is close to fixation (orange and red spots) is notably reduced (cf. fig. 1*d*). The clusters of low frequencies of allele *B* are also smaller. Clusters of fixation or low frequencies of allele *B* are located at the same approximate positions as the corresponding clusters of fixation or low frequencies of allele *A*.

Increasing values of prevalence of mutualistic sites ($p = 0.50$) lead to a significant increase in the characteristic sizes of clusters of fixation of allele *B* (red spots). However, even with the largest value considered for gene flow ($m = 0.050$; fig. 2*h*), polymorphic clusters are still present on a large portion of the landscape when mutualistic and antagonistic sites are equally prevalent. Several small clusters of low frequencies of allele *B* (blue spots) are also present in this scenario. These clusters were not observed for allele *A* under the same values for the proportion of mutualistic sites, *p*, and gene flow, *m* (fig. 1*h*). Overall, when mutualistic sites are highly prevalent ($p = 0.75$), complete landscape-wide fixation of allele *B* is not accomplished even for the highest value of gene flow (fig. 2*l*).

When scaled up into large landscapes, our modeling approach shows effects and patterns that substantially deviate from the theoretical predictions derived from two-site models in two fundamental ways. First, even for high rates of gene flow, local antagonistic clusters shield the effects of mutualisms, thereby leading to local aggregations of populations where alleles *A* and *B* are not fixed (yellow spots in fig. 1*g*, 1*h*, 1*k*; see also fig. 2*l*). Second, unlike in two-site models, sites with low frequencies of alleles *A* and *B* can occur (blue spots in fig. 1*c*, 1*d*; see also fig. 2*h*, 2*k*), even though the initial frequencies of these alleles are higher than those of alleles *a* and *b* for all the sites. In these large landscapes, the average size of these blue spots changes for different rates of gene flow (see video A1 in the appendix).

Patterns of Host's Local Adaptation in Coevolutionary and Single-Species Models

To separate the roles played by the underlying spatial mosaic structure (mutualistic and antagonistic sites' spatial distributions) and by the coevolutionary dynamics on the final phenotypic patterns, we next fixed $x_{ij} = 1$ throughout the landscape (allele *A* fixed in all sites). This is analogous to a local adaptation model for one species (Lenormand 2002), in which allele *B* has a fitness $1 + |K_M|$ at the sites assigned for mutualism and fitness $1 - |K_A|$ at sites assigned for antagonism (allele *b* has fitness 1 in all sites). We used the same selection mosaics used in figures 1 and 2 and compared the patterns obtained for the single-species model (fig. 3) with

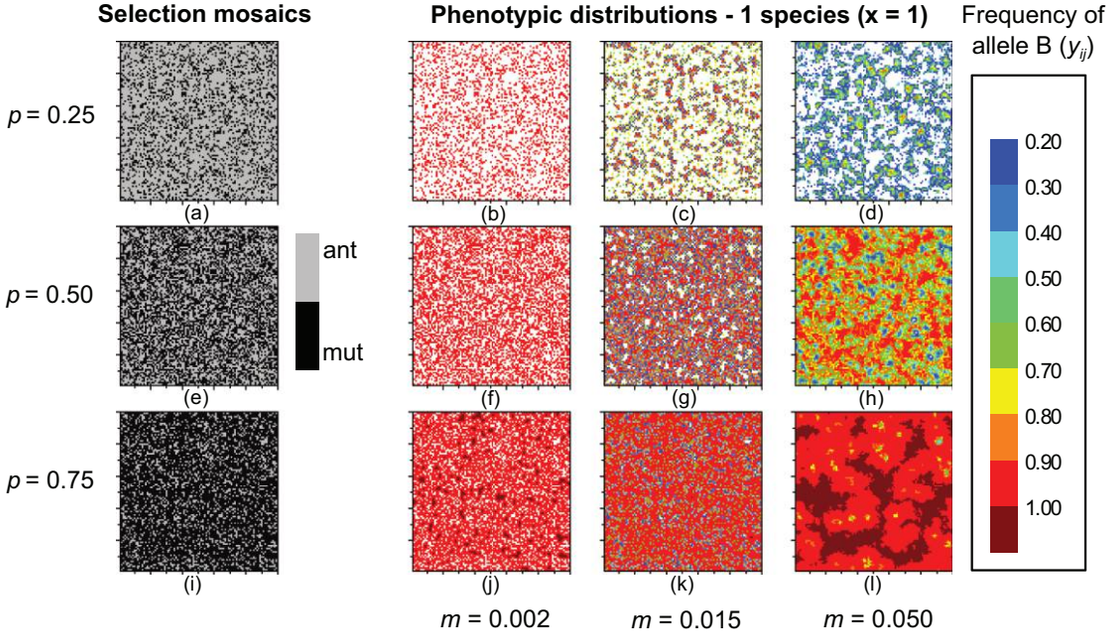

Figure 3: Final stationary patterns of *y* (frequency of allele *B*), corresponding to the single-species model (frequency of allele *A* is fixed as $x = 1$ at all sites), for three rates of gene flow, *m*, and different selection mosaics, with probability *p* for sites where selection is beneficial. Sites where selection is detrimental (fitness of allele *B* equals $1 - |K_A|$) or beneficial (fitness of allele *B* equals $1 + |K_M|$), correspond to the position of antagonistic (ant) or mutualistic (mut) sites, respectively, on the mosaics of figures 1 and 2. Parameters are the same as used in the previous figures. Each simulation ran for 40,000 generations.

the ones obtained for the two-species coevolutionary model (fig. 2). As the proportion of mutualistic sites on the landscape reaches high values ($p = 0.50$ and 0.75), increasing gene flow makes the patterns for allele *B* on the single-species model nearly identical to the patterns for the coevolutionary model. This occurs because, at this high proportion of mutualistic sites and with $|K_M| = 2|K_A|$, high rates of gene flow lead to a nearly complete fixation of allele *A* on the landscape (fig. 1*h*, 1*l*).

For a low level of mutualistic prevalence on the landscape ($p = 0.25$), the distinction between the patterns is more clearly noted. For the coevolutionary model, the antagonistic sites tend to a state of polymorphism between alleles *B* and *b* (fig. 2*a*–2*c*), whereas for the single-species model, the sites where allele *b* has a fitness advantage over allele *B* (which are exactly the antagonistic sites on the previous model) reach a state of fixation or near fixation of allele *b* (white sites; fig. 3*a*–3*c*). For high levels of gene flow, the position and shape of the clusters of high allele *B* frequency (yellow and orange sites) are similar in both cases (figs. 2*d*, 3*d*), indicating that the spatial structure of the selection mosaic influences the spatial arrangement of the final pattern. Nevertheless, the dynamics underlying the coevolutionary version of the model play a fundamental role in determining the regions of polymorphism or allele fixation.

The coevolutionary model results in less spatial structure than the single-species model with respect to the landscape-wide polymorphic pattern (fig. 2*d*), as many of the mutualistic sites tend to the polymorphic state for high gene flow. It is still possible to more easily distinguish the sites for which selection is beneficial or detrimental for allele *B* on the single-species model, since the sites in which selection is beneficial for *B* resist fixation of *b* (cf. blue sites in fig. 3*d* with structure of the mosaic in fig. 3*a*).

Gene Flow, Spatial Structure, and Coldspots

We next explored how information is transferred from selection acting in one species (mutualistic or antagonistic selection on the host) to phenotypic evolution on the other (symbiont) species as a result of the interaction by focusing our attention on the patterns obtained for allele *A*. We analyzed the effects of gene flow, spatial selection structure, and the presence of evolutionary coldspots on these final patterns.

As the proportion of mutualistic sites increases, the relationship between gene flow and the fraction of sites near fixation of allele *A* changes from hump shaped to a monotonic increase (fig. 4*a*). For $p = 0.25$ and starting with small values of *m*, increasing gene flow results in an initial tendency of increasing the number of sites showing fixation of allele *A*. However, this locally strong influence of mutualism is compensated by the spatial prevalence of antagonistic sites, leading the majority of sites to retain polymorphism for higher values of gene flow. This hump-shaped relationship is also seen for $p = 0.30$, although the decay toward polymorphism for increasing values of gene flow is slower. For higher values of *p*, increasing values of gene flow always leads to increasing values of the fraction of sites with allelic frequencies of *A* near to fixation. For $p = 0.50$ or higher, even for intermediate values of gene flow a significant fraction of the lattice presents high values of the frequency of *A* (cf. fig. 1*g*, 1*k*).

The combined effects of the proportion of mutualistic sites, the relative strengths of mutualistic and antagonistic selection, and gene flow create two possible behaviors for the ten-

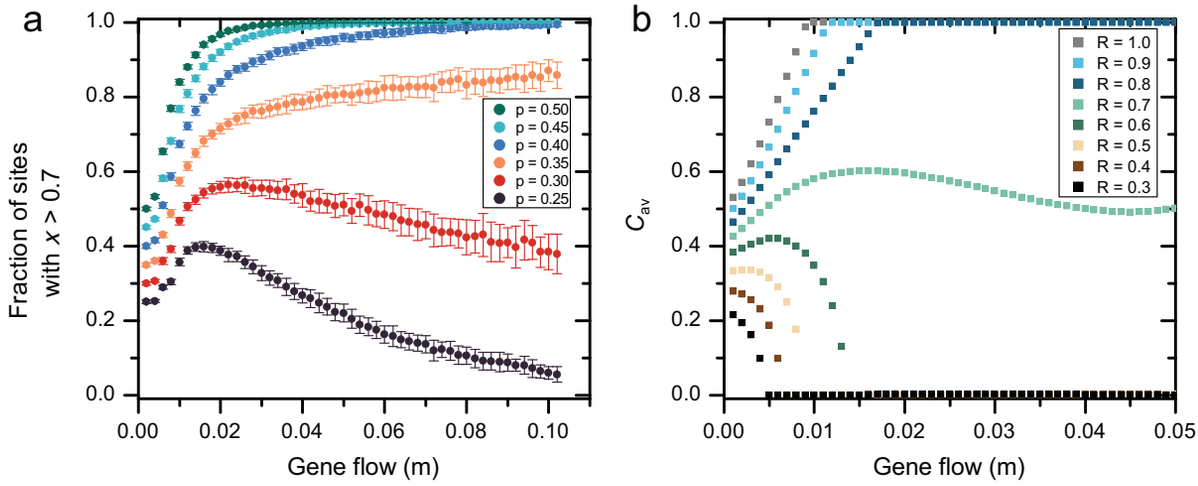

Figure 4: *a*, Average fraction of sites on the lattice for which $x > 0.7$ as a function of the gene flow *m*, for different values of the proportion of mutualistic sites, *p*. For each value of *m*, 50 samples were considered and error bars correspond to 1 SD. *b*, Results for the mean-field approach, with values of C_{av} as a function of the gene flow *m*, for different size ratios of mutualistic to antagonistic communities, $R = N_1/N_2$.

dency to fixation of allele *A* (fig. 4*a*). One is a monotonic increase in the fraction of near-to-fixation sites, as gene flow increases, until all lattice presents the same phenotypic patterns (for $p > 0.35$). The other is an initial increase of the fraction of near-to-fixation sites with subsequent decrease, leading to the polymorphic state, for high rates of gene flow (for $p < 0.30$). These outcomes suggest the existence of a threshold value for p, which would mark the transition between these different scenarios. Indeed, we derived the expression that shows that the transition between the tendency to polymorphism versus the tendency to allelic fixation, as gene flow increases, is governed by the value of the average sensitivity experienced by the host species, $\overline{s_Y}$ (see eq. [A3]). When $\overline{s_Y}$ is negative, the landscape tends to polymorphism for large values of gene flow, whereas it tends to fixation when $\overline{s_Y}$ is positive. For the values of interaction strengths used ($K_M = 0.04$ and $K_A = -0.02$), the transition between these two tendencies occurs at $p = 0.33$, when $\overline{s_Y} = 0$ (see eq. [A3]).

The tendency toward fixation or polymorphism is also observed in the mean-field model (fig. 4*b*). When both communities have the same size ($R = 1$), the larger selective strength of mutualism compared to antagonism is enough to spread the tendency toward fixation (i.e., C_{av} approaches one), which characterizes the mutualistic community. If the size of the mutualistic community is slightly reduced, for $R \geq 0.8$, the pattern still tends toward fixation as gene flow increases. In these cases, the strength of the mutualistic interaction has a stronger effect when compared to community size. Further reductions in the size of the mutualistic community lead to a drastic change in the behavior of the system, with both communities tending toward polymorphism ($C_{\text{av}} = 0$) as the gene flow increases when $R \leq 0.60$.

The results of the mean-field approach are therefore qualitatively similar to those obtained for the spatial case, with a clear transition between two states of allelic diversity. In addition, the two frameworks (spatial and mean field) also suggest that even under strong mutualistic selection and high gene flow, polymorphisms can persist. In the spatial model, persistence occurs if antagonistic sites are predominant across the landscape when considering all sites or, in the case of the mean field, if the size of the antagonistic community is greater than the size of the mutualistic community. However, the value of R that seems to mark the transition between the two behaviors on the mean-field model ($R \approx 0.7$) is not exactly the same that would be expected through direct comparison with the value of p for the transition on the lattice model (in eq. [8], for $p = 1/3$ one would expect $R = 0.5$). Even though an exact quantitative comparison with the spatial case is not possible in this approximation, the mean-field model succeeds in depicting a transition between two possible coevolutionary outcomes, similar to that found on the spatial case.

A closer analysis of the size of mutualistic clusters suggests a relationship between the structure of the geographic selection mosaic (i.e., the distribution and the relative proportion of mutualistic and antagonistic sites) and the size of phenotypic clusters. In the absence of gene flow, the frequencies of clusters with high allele frequency coincide with the frequencies of mutualistic clusters for both *A* and *B* (fig. 5*a*, 5*b*). Increasing gene flow increases not only the mean cluster size but also the probability of finding a cluster of allele fixation larger than expected from the spatial distribution of mutualistic sites (fig. 5). However, a clear distinction can be noted on the changes in cluster frequencies for alleles *A* and *B* as gene flow increases. As shown before for the spatial patterns (figs. 1, 2), the characteristic sizes of the clusters where the frequency of allele *B* is close to fixation (>0.7) is smaller than sizes of clusters on the same interval for allele *A* for the same gene flow rate. The interval of sizes of clusters close to fixation is also significantly broader for allele *A* (fig. 5*a*) for all values of gene flow. Important differences in cluster frequencies can also be shown when comparing allele *B* frequencies on the coevolutionary and single-species models (see figs. A5, A6; figs. A1–A6 are available online).

From the results of cluster frequencies (fig. 5), we note that fixation of alleles throughout a landscape depends on the combined effects of the spatial distribution of mutualistic and antagonistic sites, forming the selection mosaics, and the rate of gene flow, also presenting important differences between interacting species. These results lead to two main predictions: first, the presence of phenotypic clusters with variable sizes across landscapes might hide the outcomes of the interactions at finer spatial scales (e.g., phenotypic clusters of allele fixation might be formed by many sites where the interaction is antagonistic). Second, the presence of phenotypic clusters with broad variation in sizes might actually be an indication that a nonregular spatial structure of small and medium-size clusters of mutualistic and antagonistic sites are shaping phenotypic evolution in a coevolutionary context (regular structures with equal sizes, even if there were many, would not allow the formation of broad distributions of phenotypes; cf. these phenotypic patterns with the ones obtained from regular block mosaics in the appendix).

Finally, we added to these large landscapes the third component of geographic mosaics: coevolutionary hotspots and coldspots. In the coevolutionary coldspots, the interaction affected the evolutionary dynamics of the symbiont but not the host (i.e., $\gamma_{ij} = 0$ representing the absence of interaction effect on fitness of species Y). In other words, coldspots represent communities where the symbiont was commensalistic on its host. We distributed coevolutionary coldspots among the antagonistic and mutualistic sites. We then explored the effects of the proportion of coldspots and the rates of gene flow on the frequency of sites with high frequencies of allele *A* ($x > 0.7$), as we kept the average fitness sensitivity of the host fixed. For fixed values of gene flow, the tendency toward allelic fixation on the symbiont depended on the av-

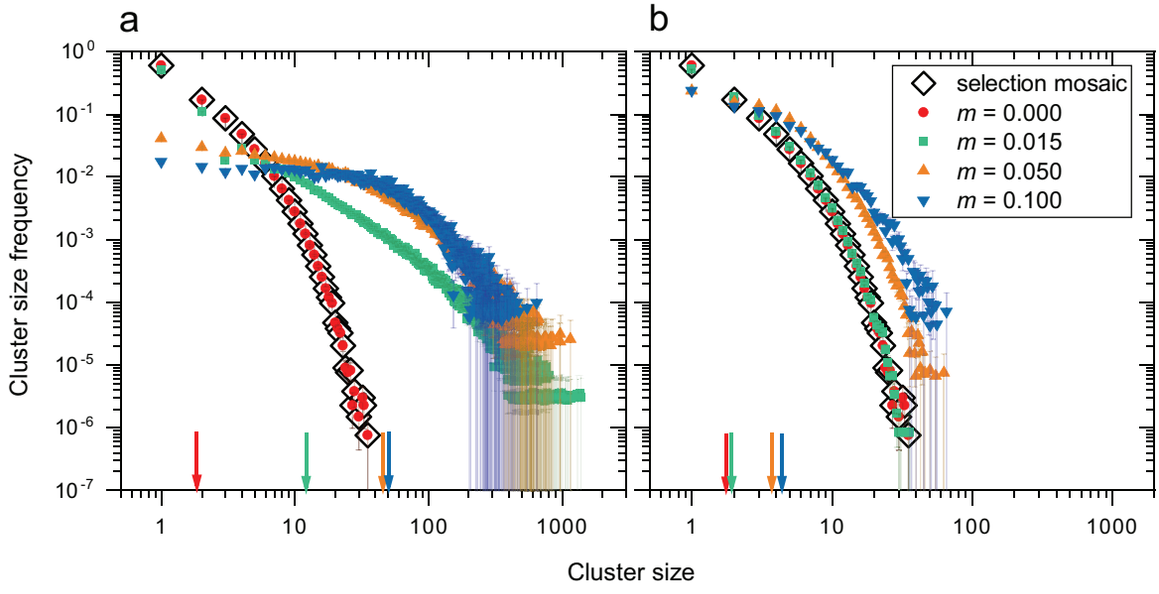

Figure 5: Cluster size frequencies for alleles *A* (*a*) and *B* (*b*) for four different values of gene flow, *m*, for the cluster of sites in which the allele frequency is greater than 0.7 (see description in "Methods"). Each point represents the number of clusters with that size normalized by the total cluster count. For each rate of gene flow, 1,000 different selection mosaics (error bars equal to the standard error of the mean) with $p = 0.25$ were considered. Open diamonds show the same cluster analysis considering the mutualistic clusters on the selection mosaic. Arrowheads represent the mean cluster size for each value of *m* (using the same color legends). As before, $K_M = 0.04$, $K_A = -0.02$, and $Q = 0.02$.

erage value of the fitness sensitivity of the host. For a negative average fitness sensitivity (fig. 6*a*), increasing the fraction of coldspots led to a decrease in the number of sites with high frequencies of allele *A*. In contrast, for a positive average fitness sensitivity (fig. 6*c*), the increase in the fraction of coldspots led to an increase in the number of sites with high allele *A* frequencies.

The effect of coldspots follows from the influence of the mutualistic clusters on the initial selection mosaics. Because the probability *p* for the initial selection mosaic is a function

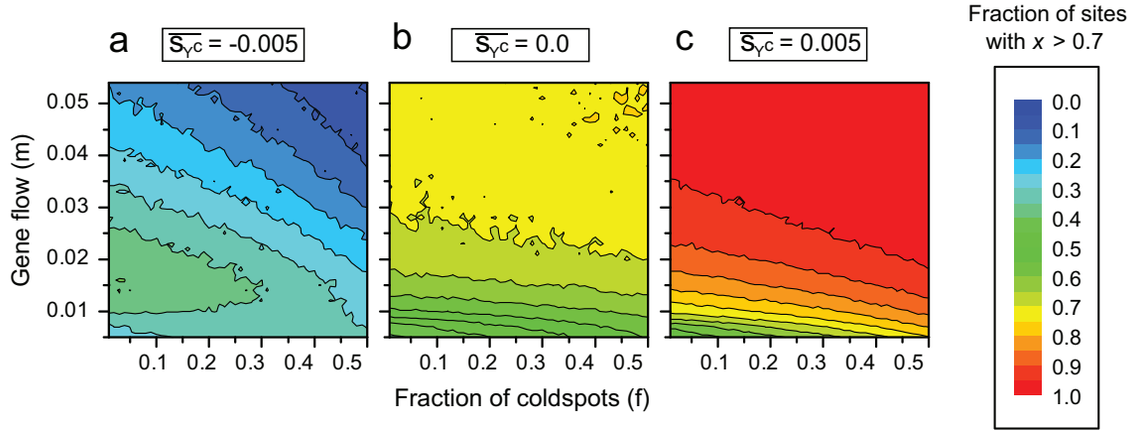

Figure 6: Average fraction of sites on the lattice that present final values $x > 0.7$ for different values of gene flow, *m*, and the fraction of coldspots, *f*, on the lattice. The average fitness sensitivity for the host, $\overline{s_{Y^C}}$, is fixed in each case, with values -0.005 (*a*), 0.0 (*b*), and 0.005 (*c*). The original lattices are constructed with *p* for the initial selection mosaic varying with *f* according to equation (9). Ten simulations for each pair (m, f) were performed. For all cases, $K_M = 0.04$, $K_A = -0.02$, and $Q = 0.02$.

of f, so that the average fitness sensitivity is fixed (see "Methods" and the appendix), the variation of p is dependent on the value of the average fitness. For $\overline{s_{YC}} < 0$ (fig. 6*a*), p is a decreasing function of f: with $\overline{s_{YC}} = -0.005$, as f increases from 0.0 to 0.5, p decreases from 0.25 to 0.17. In contrast, for $\overline{s_{YC}} > 0$ (fig. 6*c*), p is an increasing function of f: with $\overline{s_{YC}} = 0.005$, as f increases from 0.0 to 0.5, p increases from 0.42 to 0.50. For $\overline{s_{YC}} = 0.0$, p is independent of f, and thus the number of sites presenting high allele A frequencies should depend only on the value of the gene flow. However, it is possible to note a slight increase in the number of sites with high allele A frequencies as f increases (fig. 6*b*). This is due mainly to the fact that the lattice is finite and the selection of coldspots is slightly biased toward antagonistic sites in this case. Hence, the proportion of coldspots in a landscape alters the outcome of the interaction in different ways that depend on the landscape proportions of mutualistic and antagonistic sites, as well as on fitness sensitivity of the interacting species.

Discussion

Previous studies have been successful in describing the evolutionary forces that drive the formation of single-species clines in traits (Nagylaki 1975; Felsenstein 1976; Slatkin 1978; Lenormand 2002). Adding to the vast literature of local adaptation in single species, subsequent studies have also investigated the formation of evolutionary clines in one-dimensional systems of coevolving species (Nuismer et al. 2000). Here we have shown that novel dynamics result when species coevolve across large landscapes over which the interactions vary from antagonism to mutualism, forming a geographic selection mosaic of ecological outcomes. These novel dynamics produce geographic clusters of similar phenotypes, resulting from a combination of the geographic mosaics, the distribution of coevolutionary hotspots and coldspots, and the degree and pattern of gene flow.

Direct comparison between the two-species and single-species models indicated that for small fractions of mutualistic sites in the landscape ($p = 0.25$), significant differences appeared for allele composition on antagonistic sites. Whereas polymorphic states are observed with notable spatial predominance in the coevolutionary case, for the single-species model polymorphism is associated with the transition between regions of near fixation of allele B and near fixation of allele b. As a consequence, major differences also appear in the cluster distributions for allele B in these two models (figs. A5, A6).

These results imply that the two main drivers for the formation of the patterns we describe are the two-dimensional topology of the selection mosaics, which influences position and size distribution of the phenotypic clusters, and coevolutionary dynamics, which directly affect the maintenance of fixation and polymorphism on the landscape. Our results therefore expand current local adaptation theory by showing that (i) a large bidimensional landscape serves as a stage for the formation of a broad size distribution of mutualistic and antagonistic clusters, which are directly linked to the formation of phenotypic clusters that nonlinearly vary in size with gene flow (see fig. 5), and (ii) maintenance of polymorphisms in large ecologically complex landscapes is significantly altered by coevolutionary dynamics and depends on the rate of gene flow and the spatial prevalence of mutualism or antagonism.

In this work, we isolated how the spatial scales of selection and gene flow affect the spatial scale of adaptation and coadaptation when interactions vary from antagonism to mutualism within a large landscape. This analysis was performed by focusing mostly on allele A, but our analyses also showed that the dynamics of allele B differ in some respects from those found in A. A deeper analysis of the patterns of allele B would also be important, as well as investigating how the mismatch between interacting alleles A and B is dependent on gene flow and spatial structure. However, these analyses introduce another set of effects that need to be evaluated in a truly robust way, which goes beyond the scope of this article.

Our results are directly relevant to understanding the structure of coevolving interactions found in nature. Selection mosaics, coevolutionary hotspots, and variable frequencies of coevolving traits have been observed in nature at a wide range of spatial scales (Thompson 2013). Moreover, geographic mosaics in coevolutionary selection have been previously shown to be an important ingredient in the formation of evolutionary patterns. For example, observed geographic mosaics range from mosaics of ecological outcomes or traits (e.g., Benkman et al. 2001; Brodie et al. 2002; Thompson and Cunningham 2002) to clinal patterns in traits, such as in the interaction between camellias (*Camellia japonica*) and camellia weevils (*Curculio camelliae*) along latitudinal and elevational gradients in Japan (Toju et al. 2011). Our work opens the opportunity to investigate the underlying processes shaping coevolving interactions in the large and more complex landscapes found in other interactions.

In one-dimensional models of geographic mosaics, the most likely outcome is the evolution of clines (Nuismer et al. 2000). Our results for the analyses of large landscapes suggest three extensions of coevolutionary theory. First, the interplay between spatial structure, gene flow, and selection mosaics can lead to the formation of clusters of allelic frequencies that differ significantly from those expected by the spatial distribution of mutualistic and antagonistic sites. On the local level, one would expect fixation of alleles on mutualistic sites and polymorphism on antagonistic sites. Our results instead show a marked discrepancy between the final allelic frequencies and that expected by local selection regimes at finer spatial scales. These results support the view

that all three components of the geographic mosaic of coevolution—selection mosaics, hotspots, and trait remixing—should be considered when investigating how species interactions shape evolution of alleles and traits (Thompson 2005). Empirical work has described the spatial structure of magnitude and direction of selection, as well as the distribution of phenotypes of several coevolved species interactions (Brodie et al. 2002; Parchman and Benkman 2002; Ruano et al. 2011). Some of these studies have revealed clusters of populations sharing similar trait patterns, in which a mismatch between phenotypic patterns and selection often occurs (Hanifin et al. 2008; Nogueira et al. 2015). Previous work associates this pattern with differences in responses of interacting species to coevolutionary selection (Hanifin et al. 2008) or to similar directional selection across space (Benkman and Parchman 2013). Our study provides an additional mechanism that may contribute to these spatial patterns: the formation of trait clusters as a consequence of gene flow amplifying local selection and generating a distribution of clusters of phenotypes.

Second, a key aspect of the disparity between the spatial distribution of the selection mosaics and the resulting phenotypes is the formation of local clustering of sites showing similar allele frequencies. We provide a mechanism for this departure in allele distributions by hypothesizing that aggregations of sites with similar selective regimes shield the effects of stronger interaction strength and/or higher prevalence of other selective regimes, leading to the formation of the phenotypic clusters. Nuismer et al. (2000) reported a shielding effect in their linear spatial model of coevolution. By generalizing coevolutionary models to two-dimensional lattices, our study shows that this shielding effect leads to the formation of clusters of multiple sizes across the landscape. Together these results suggest that shielding effects may be a common feature of coevolution for interactions with a geographic mosaic structure. The comparison with the mean-field results also suggests the relevance of numerical effects and spatial structure to understanding these final distributions of phenotypes. These analyses suggest that coevolution across space favors the formation of discrete regional groups of populations sharing similar phenotypes, even if selection mosaics are not spatially organized. In this sense, the statistical properties of the distribution of cluster sizes provide information on the role of gene flow in reshaping the patterns of traits predicted by selection mosaics. Additionally, our model predicts a wide variation in cluster sizes within metapopulations of interacting species, in agreement with empirical evidence supporting the notion that cluster patterns in traits and allele frequencies can occur on scales varying from a few square kilometers or less (King et al. 2009; Laine 2009; Koskella et al. 2011) to scales of tens or hundreds of square meters or more (Anderson and Johnson 2008; Hanifin et al. 2008; Pennings et al. 2009; Benkman et al. 2010; Burdon and Thrall 2014).

Third, we show that coevolutionary coldspots may change evolutionary dynamics by modulating the effects of gene flow, favoring particular allele frequencies and changing the consequences of the selection mosaics. Recent work shows that the spatial organization of coldspots and hotspots affects the polymorphism persistence in small spatial networks of two antagonistic species (Gibert et al. 2013). By incorporating the fact that mutualisms and antagonisms are often the end points of a continuum of variable fitness consequences (Thompson 2005), the asymmetry in selection that characterizes coldspots favors an asymmetry of the distribution of alleles at the landscape level, thereby maintaining allele diversity (and polymorphism) in the host populations over large spatial areas.

More generally, the results suggest how future theoretical and empirical studies could explore the statistical properties of cluster of traits and selection mosaics within metapopulations of interacting species. Selection mosaics incorporated into metacommunity structure show that central communities might play a disproportionate role in coevolutionary dynamics (Lemos-Costa et al. 2017). When scaled up to the landscape level, we hypothesize that the spatial effects described here will amplify the formation of clusters of high or low allele frequencies in nature. The formation of discrete regional groups is a form of a broad class of spatial processes that occur in biological and physical systems (Alonso et al. 2002; Liu et al. 2010). In this sense, this work represents a step in creating a bridge between coevolutionary theory (Thompson 2005) and the study of spatial processes in dynamical systems (Murray 2011).

We have incorporated two important simplifying assumptions in our model, namely, infinite population sizes and haploid organisms. Infinite population sizes enable us to work exclusively with gene frequencies, focusing our analysis on the dynamical effects of frequency-dependent selection and controlling for the stochasticity inherent to finite population sizes. It is important to note that this assumption holds as long as the number of migrants is small compared to the local populations on a finite case. If the number of migrants is large, dynamical instabilities associated with the formation of the final patterns would likely lead to dynamical regimes different from the stationary patterns discussed here. A robust analysis of these regimes, considering demographic dynamics of varying population sizes in space and consequently asymmetric rates of gene flow, would be an important extension of our work that would permit an understanding of how eco-evolutionary dynamics affect the spatial distribution of phenotypes. Additionally, diploid traits might introduce an additional source of local diversification even under the influence of strong mutualistic selection, which has been shown to prevent diversification in many cases (Raimundo et al. 2014).

Finally, these results provide a framework for future studies to explore the coevolutionary consequences of human-

driven habitat fragmentation and loss in natural landscapes. Although we focus mainly on the final stationary patterns of allelic distributions, the transient evolutionary dynamics are important and relevant, especially nowadays as environments worldwide are undergoing rapid change. The results of this study also reinforce the difficulty of interpreting the spatial structure of interaction outcomes and future trajectories in coevolving interactions based on analyses focusing only on local and small-scale allele frequencies, even after hundreds of generations. For now, we predict that habitat fragmentation, by reducing rates of gene flow across landscapes, is likely to impede the formation of larger clusters of populations with similar phenotypes, thereby making the spatial structure of phenotypes (distribution of phenotypic clusters) more similar to the structure of selection mosaics (clusters of mutualism or antagonism).

Acknowledgments

We acknowledge the funding provided by the European Union Seventh Framework Programme (FP7/2007–2013; grant agreement 289384 [L.D.F.]), the São Paulo Research Foundation (grants 2009/54422-8 [P.R.G.], 2016/06054-3 [M.A.M.A.], and 2015/26989-4 [L.D.F.]), the National Council of Scientific and Technological Development (M.A.M.A. and P.L.-C.), and the National Science Foundation (DEB-0839853 [J.N.T.]).

Literature Cited

Alonso, D., F. Bartumeus, and J. Catalan. 2002. Mutual interference between predators can give rise to Turing spatial patterns. Ecology 83: 28–34.

Anderson, B., and S. D. Johnson. 2008. The geographical mosaic of coevolution in a plant-pollinator mutualism. Evolution 62:220–225.

Benkman, C. W., W. C. Holimon, and J. W. Smith. 2001. The influence of a competitor on the geographic mosaic of coevolution between crossbills and lodgepole pine. Evolution 55:282–294.

Benkman, C. W., and T. L. Parchman. 2013. When directional selection reduces geographic variation in traits mediating species interactions. Ecology and Evolution 3:961–970.

Benkman, C. W., T. L. Parchman, and E. T. Mezquida. 2010. Patterns of coevolution in the adaptive radiation of crossbills. Annals of the New York Academy of Sciences 1206:1–16.

Brodie, E. D., B. J. Ridenhour, and E. D. Brodie III. 2002. The evolutionary response of predators to dangerous prey: hotspots and coldspots in the geographic mosaic of coevolution between garter snakes and newts. Evolution 56:2067–2082.

Burdon, J. J., and P. H. Thrall. 2014. What have we learned from studies of wild plant-pathogen associations? the dynamic interplay of time, space and life-history. European Journal of Plant Pathology 138:417–429.

Dybdahl, M. F., and C. M. Lively. 1996. The geography of coevolution: comparative population structures for a snail and its trematode parasite. Evolution 50:2264–2275.

Felsenstein, J. 1976. The theoretical population genetics of variable selection and migration. Annual Review of Genetics 10:253–280.

Forde, S. E., J. N. Thompson, and B. J. M. Bohannan. 2004. Adaptation varies through space and time in a coevolving host-parasitoid interaction. Nature 431:841–844.

Gandon, S., A. Buckling, E. Decaestecker, and T. Day. 2008. Host-parasite coevolution and patterns of adaptation across time and space. Journal of Evolutionary Biology 21:1861–1866.

Gibert, J. P., M. M. Pires, J. N. Thompson, and P. R. Guimarães. 2013. The spatial structure of antagonistic species affects coevolution in predictable ways. American Naturalist 182:578–591.

Gómez, J. M., F. Perfectti, J. Bosch, and J. P. M. Camacho. 2009. A geographic selection mosaic in a generalized plant-pollinator-herbivore system. Ecological Monographs 79:245–263.

Gómez, P., and A. Buckling. 2011. Bacteria-phage antagonistic coevolution in soil. Science 332:106–109.

Gomulkiewicz, R., J. Thompson, R. Holt, S. Nuismer, and M. Hochberg. 2000. Hot spots, cold spots, and the geographic mosaic theory of coevolution. American Naturalist 156:156–174.

Gotelli, N. J., G. R. Graves, and C. Rahbek. 2010. Macroecological signals of species interactions in the Danish avifauna. Proceedings of the National Academy of Sciences of the USA 107:5030–5035.

Guimarães, P. R., M. M. Pires, P. Jordano, J. Bascompte, and J. N. Thompson. 2017. Indirect effects drive coevolution in mutualistic networks. Nature 550:511.

Hanifin, C. T., E. D. Brodie Jr., and E. D. Brodie III. 2008. Phenotypic mismatches reveal escape from arms-race coevolution. PLoS Biology 6:e60.

Johnson, S. D. 2010. The pollination niche and its role in the diversification and maintenance of the southern African flora. Philosophical Transactions of the Royal Society B 365:499–516.

King, K. C., L. F. Delph, J. Jokela, and C. M. Lively. 2009. The geographic mosaic of sex and the Red Queen. Current Biology 19:1438–1441.

Koskella, B., J. N. Thompson, G. M. Preston, and A. Buckling. 2011. Local biotic environment shapes the spatial scale of bacteriophage adaptation to bacteria. American Naturalist 177:440–451.

Laine, A.-L. 2009. Role of coevolution in generating biological diversity: spatially divergent selection trajectories. Journal of Experimental Botany 60:2957–2970.

Lemos-Costa, P., A. B. Martins, J. N. Thompson, and M. A. de Aguiar. 2017. Gene flow and metacommunity arrangement affects coevolutionary dynamics at the mutualism-antagonism interface. Journal of the Royal Society Interface 14:20160989.

Lenormand, T. 2002. Gene flow and the limits to natural selection. Trends in Ecology and Evolution 17:183–189.

Lexer, C., C. Caseys, C. Stritt, and T. G. Whitham. 2013. Integrating the "genomic mosaic" view of species into studies of biotic interactions: a comment on Bernhardsson et al. (2013). Ecology Letters 16:1515–e7.

Lion, S., and S. Gandon. 2015. Evolution of spatially structured host-parasite interactions. Journal of Evolutionary Biology 28:10–28.

Liu, Q.-X., R.-H. Wang, Z. Jin, J. van de Koppel, and D. Alonso. 2010. Spatial self-organization in a multi-strain host-pathogen system. Journal of Statistical Mechanics: Theory and Experiment 2010:P05017.

Murray, J. 2011. Mathematical biology. Vol. II. Spatial models and biomedical applications. Interdisciplinary Applied Mathematics. Springer, New York.

Nagylaki, T. 1975. Conditions for the existence of clines. Genetics 80:595–615.

Nogueira, A., P. J. Rey, J. M. Alcántara, R. M. Feitosa, and L. Lohmann. 2015. Geographic mosaic of plant evolution: extrafloral nec-

tary variation mediated by ant and herbivore assemblages. PLoS ONE 10:e0123806.
Nuismer, S. L., P. Jordano, and J. Bascompte. 2013. Coevolution and the architecture of mutualistic networks. Evolution 67:338–354.
Nuismer, S. L., J. N. Thompson, and R. Gomulkiewicz. 1999. Gene flow and geographically structured coevolution. Proceedings of the Royal Society B 266:605–609.
———. 2000. Coevolutionary clines across selection mosaics. Evolution 54:1102–1115.
Parchman, T. L., and C. W. Benkman. 2002. Diversifying coevolution between crossbills and black spruce on Newfoundland. Evolution 56:1663–1672.
Pennings, S. C., C. K. Ho, C. S. Salgado, K. Wieski, N. Davé, A. E. Kunza, and E. L. Wason. 2009. Latitudinal variation in herbivore pressure in Atlantic Coast salt marshes. Ecology 90:183–195.
Raimundo, R. L. G., J. P. Gibert, D. H. Hembry, and P. R. Guimarães. 2014. Conflicting selection in the course of adaptive diversification: the interplay between mutualism and intraspecific competition. American Naturalist 183:363–375.
Rice, S. H. 2004. Evolutionary theory: mathematical and conceptual foundations. Sinauer, New York.
Ruano, F., S. Devers, O. Sanllorente, C. Errard, A. Tinaut, and A. Lenoir. 2011. A geographical mosaic of coevolution in a slave-making host-parasite system. Journal of Evolutionary Biology 24:1071–1079.
Slatkin, M. 1978. Spatial patterns in the distributions of polygenic characters. Journal of Theoretical Biology 70:213–228.
Thompson, J. N. 2005. The geographic mosaic of coevolution. Interspecific Interactions. University of Chicago Press, Chicago.
———. 2013. Relentless evolution. University of Chicago Press, Chicago.
Thompson, J. N., and B. M. Cunningham. 2002. Geographic structure and dynamics of coevolutionary selection. Nature 417:735–738.
Thompson, J. N., and K. F. Merg. 2008. Evolution of polyploidy and the diversification of plant-pollinator interactions. Ecology 89:2197–2206.
Toju, H., H. Abe, S. Ueno, Y. Miyazawa, F. Taniguchi, T. Sota, and T. Yahara. 2011. Climatic gradients of arms race coevolution. American Naturalist 177:562–573.
van Valen, L. 1973. A new evolutionary law. Evolutionary Theory 1:1–30.
Vogwill, T., A. Fenton, A. Buckling, M. E. Hochberg, and M. A. Brockhurst. 2009. Source populations act as coevolutionary pacemakers in experimental selection mosaics containing hotspots and coldspots. American Naturalist 173:E171–E176.
Wade, M. J. 2007. The co-evolutionary genetics of ecological communities. Nature Reviews Genetics 8:185–195.
Whitham, T. G., J. K. Bailey, J. A. Schweitzer, S. M. Shuster, R. K. Bangert, C. J. LeRoy, E. V. Lonsdorf, et al. 2006. A framework for community and ecosystem genetics: from genes to ecosystems. Nature Reviews Genetics 7:510–523.

Associate Editor: Greg Dwyer
Editor: Judith L. Bronstein

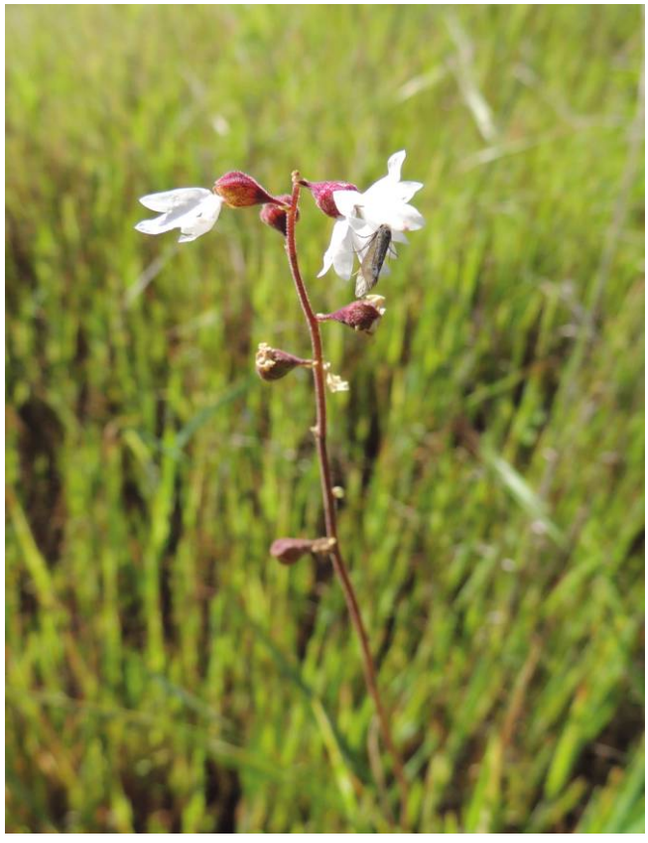

Greya obscura nectaring in *Lithophragma affine*. Photo taken at Pinnacles National Park (California, USA) in March 2016. Photo credit: Paula Lemos-Costa.